

# Prediction of Smoke Propagation in a Big Multi-Story Building Using Fire Dynamics Simulator (*FDS*)

Ahmed Farouk Abdel Gawad, Hamza Ahmed Ghulman

Mechanical Engineering Department, College of Engineering and Islamic Architecture, Umm Al-Qura Univ., Makkah, Saudi Arabia

## Email address:

afaroukg@yahoo.com (A. F. AbdelGawad)

## To cite this article:

Ahmed Farouk Abdel Gawad, Hamza Ahmed Ghulman. Prediction of Smoke Propagation in a Big Multi-Story Building Using Fire Dynamics Simulator (*FDS*). *American Journal of Energy Engineering*. Special Issue: Fire, Energy and Thermal Real-life Challenges. Vol. 3, No. 4-1, 2015, pp. 23-41. doi: 10.11648/j.ajee.s.2015030401.12

---

**Abstract:** In the present work, the computational fluid dynamics (*CFD*) technique was used to predict the fire dynamics in a big three-story building. Important aspects of fire dynamics were investigated such as smoke propagation and temperature distribution. The study aims to decrease the fire hazards by computationally predicting the expected smoke movement in real-life conditions. Consequently, early evacuation plans can be established to save human lives by proper estimation of the smoke direction and density. Also, temperature rise has a potential effect on the safety of both humans and structures. Different factors were considered such as fire location, doors, and emergency openings. Important findings and notable conclusions are recorded.

**Keywords:** Fire Dynamics, Smoke Propagation, Computational Method, Unsteady Solution

---

## 1. Introduction

### 1.1. Importance

Due to the development of modern life, people may gather at the same time and place with intensive density. This situation may initiate series fires that lead to massive losses in human lives. Commonly, most of the deaths in fires are not due to direct fire, but because of suffocation with smoke, fumes and toxic gases. Usually, the lack of experience and awareness of individuals results in the increased risk and mortality rates.

Computational prediction of the most probable direction of smoke propagation assists to save human lives. Moreover, smoke-control schemes and evacuation plans can be established as part of the fire-safety strategy.

Examples of buildings where smoke prediction and control play a remarkable role include: holy and worship places, university campuses, shopping centers, big hotels, atrium buildings, large warehouse and industrial buildings, underground structures (car parks and tunnels), *etc.*

Usually, prediction and control of smoke flow within a building may cover one or more of the following objectives: (i) Assisting fire fighting, (ii) Guarantee safe flees for the occupants of the building, (iii) Protecting property.

### 1.2. Previous Investigations

The problem of fire dynamics simulation was investigated by many researchers. Men *et al.* [1] used large eddy simulations for studying fire-driven flows. Kashef *et al.* [2] carried out computational simulations of in-situ fire tests in road tunnels. Xin *et al.* [3] investigated computationally the turbulent buoyant flame using a mixture-fraction-based combustion model. Jahn *et al.* [4] concerned the effect of model parameters on the simulation of fire dynamics. Huo *et al.* [5] considered the locations of diffusers on air flow field in an office. Razdolsky [6] investigated mathematically the modeling of fire dynamics. Cheng and Hadjisophocleous [7] considered the dynamic modeling of fire spread in buildings. Ling and Kan [8] carried out numerical simulations on fire and analysis of the spread characteristics of smoke in a supermarket. Yang *et al.* [9] investigated both experimentally and numerically a storehouse fire accident. Zhang and Li [10] studied the thermal actions in localized fires in large enclosures. Sun *et al.* [11] investigated the progressive collapse analysis of steel structures under fire conditions. Wu and Chen [12] considered 3D spatial information for fire-fighting search and rescue route analysis within buildings. Agarwal and Varma [13] studied the fire-induced progressive collapse of steel building structures.

Other investigators used fire dynamic simulator (*FDS*) code in their research work. He and Jiang [14] used *FDS* to

assess effectiveness of air sampling-type detector for the protection of large open spaces. Webb [15] used *FDS* modeling for hot smoke testing in cinema and airport concourses. Smardz [16] validated *FDS* for forced and natural convection flows. Sun *et al.* [17] evaluated the fire-plume properties with *FDS* and the Clark coupled wildfire model. Coyle and Novozhilov [18] validated *FDS* using smoke management studies. Zhang *et al.* [19] assessed *FDS* predictions for heat flux and flame heights from fires in *SBI* tests.

Moreover, smoke propagation in buildings and structures was considered by many researchers. Wu *et al.* [20] proposed a distributed method for predicting building fires based on a two-layer zone model. Zhang and Wang [21] carried out a numerical simulation of smoke movement in vertical shafts during a high-rise building fire. Jiang *et al.* [22] modeled fire-induced radiative heat transfer in smoke-filled structural cavities. Yu *et al.* [23] studied the smoke control strategy due to fire in a high-rise building. Zhang *et al.* [24] extended the work of [21] using a modified network model. Bae *et al.* [25] developed a network-based program for unsteady smoke simulation in high-rise buildings.

Also, some investigators concerned the fire evacuation simulation. Tingyong *et al.* [26] studied the building fire evacuation based on continuous model of *FDS & EVAC* code. Tang and Ren [27] carried out *GIS*-based *3D* evacuation simulation for indoor fire. Zhang *et al.* [28] modeled and analyzed *3D* complex building interiors for effective evacuation simulations.

### 1.3. Present Investigation

The present study is based on the computational fluid dynamics (*CFD*) technique using Fire Dynamic Simulator (*FDS*,v.5). This code was developed and published by the National Institute of Standards and Technologies (*NIST*), U.S. Department of Commerce [29]. The study concerns the smoke propagation due to sample fires in a big three-story building. Different factors were considered such as fire location, doors, and emergency openings. Actually, this investigation is an extension of [30]. Smokeview [31-33] was used to represent the results of the present study as will be shown in the coming sections.

## 2. Governing Equations and *LES* Simulation

### 2.1. General Features of the Computational Modeling

*FDS* code [29] is a computational tool for the prediction of fire scenarios and smoke spread that are expected in almost all types of buildings. The code prediction depends on the architectural plans of the building in addition to the burning materials. The code is based on the solution of the governing equations of flow and combustion due to fire. The core algorithm of *FDS* is an explicit predictor-corrector scheme, second-order accurate in space and time. Turbulence is

treated by means of the Smagorinsky form of Large Eddy Simulation (*LES*). More details of the *FDS* code can be found in [34,35]. There is a big number of attempts for the validation of *FDS*. Some of them are illustrated in Sec. 1.2 and many others in [36]. The validation process may be carried out using the results of other *CFD* programs, codes and standards [29, 37-43], and/or experiments as shown in Fig. 1 that illustrates a typical hot-smoke test layout using smoke canister [15]. Generally, based on these validation investigations, the results of *FDS* can be trusted for almost all fire cases; providing a fine mesh is used to model the problem under-investigation.

### 2.2. Flow Governing Equations

*FDS* solves numerically a form of the Navier-Stokes equations appropriate for low-speed; thermally-driven flow with an emphasis on smoke and heat transport from fires [16] as follows:

Conservation of mass:

$$\frac{\partial \rho}{\partial t} + \nabla \cdot \rho u_i = 0 \quad (1)$$

Conservation of momentum:

$$\frac{\partial}{\partial t} (\rho u_i) + \nabla \cdot \rho u_i u_j + \nabla p = \rho f + \nabla \cdot \tau_{ij} \quad (2)$$

Conservation of energy:

$$\frac{\partial}{\partial t} (\rho h) + \nabla \cdot \rho h u_i = \frac{Dp}{Dt} + \dot{q}''' - \nabla \cdot q + \Phi \quad (3)$$

Equation of state for a perfect gas:

$$p = \rho R T \quad (4)$$

In terms of the mass fractions of the individual gaseous species, the mass conservation equation can be written as:

$$\frac{\partial}{\partial t} (\rho Y_i) + \nabla \cdot \rho Y_i u = \nabla \cdot \rho D_i \nabla Y_i + \dot{m}_i''' \quad (5)$$

Where,  $u_i$  is velocity in  $i$ -direction,  $i=1, 2, 3$ ,  $\rho$  is fluid density,  $f$  is summation of external forces,  $\tau_{ij}$  is shear stresses,  $p$  is pressure,  $h$  is enthalpy,  $\dot{q}'''$  is heat release rate per unit volume (*HRRPUV*),  $q$  is the heat transfer,  $\Phi$  is any heat source, and  $T$  is the temperature.  $Y_i$  is the mass fraction.

### 2.3. Large Eddy Simulations (*LES*) and Sub-Grid Scale Models

Large eddy simulation resolves large scales of the flow field solution allowing better fidelity than alternative approaches such as Reynolds-averaged Navier-Stokes (*RANS*) methods. It also models the smallest scales of the solution, rather than resolving them as direct numerical simulation (*DNS*) does.

For incompressible flow, the continuity equation and

Navier-Stokes equations are filtered, yielding the filtered incompressible continuity equation,

$$\frac{\partial \bar{u}_i}{\partial x_i} = 0 \quad (6)$$

and the filtered Navier-Stokes equations,

$$\frac{\partial \bar{u}_i}{\partial t} + \frac{\partial}{\partial x_j} (\bar{u}_i \bar{u}_j) = -\frac{1}{\rho} \frac{\partial \bar{p}}{\partial x_i} + \nu \frac{\partial^2 \bar{u}_i}{\partial x_j \partial x_j} - \frac{\partial}{\partial x_j} \tau_{ij} \quad (7)$$

Where,  $\bar{p}$  is the filtered pressure field and  $\tau_{ij} = \bar{u}_i \bar{u}_j - \bar{u}_i \bar{u}_j$  is the subgrid-scale stress tensor.  $\tau_{ij}$  is found by an eddy viscosity representation for small scales as [44]:

$$\tau_{ij} = \frac{1}{3} \tau_{kk} \delta_{ij} = -2 \nu_T \bar{S}_{ij} \quad (8)$$

Where,  $\delta_{ij}$  is the Kronecker's delta. To find  $\tau_{ij}$ , the Smagorinsky-Lilly sub-grid scale *SGS* model, which was developed by Smagorinsky [45] and used in the first *LES* simulation by Deardorff [46], is used.

The eddy viscosity is modeled as:

$$\nu_T = (C_s \Delta_g)^2 \sqrt{2 \bar{S}_{ij} \bar{S}_{ij}} = (C_s \Delta_g)^2 |S| \quad (9)$$

Where,  $\Delta_g$  is the filter width that is calculated as:

$$\Delta_g = (\Delta_x \Delta_y \Delta_z)^{1/3} \quad (10)$$

$\Delta_x$ ,  $\Delta_y$  and  $\Delta_z$  are the grid sizes in the three Cartesian coordinates  $x$ ,  $y$  and  $z$ , respectively.  $C_s$  is a modeling constant that is problem-dependent. The magnitude of the large-scale strain rate tensor is defined as:

$$\bar{S}_{ij} = \frac{1}{2} \left( \frac{\partial \bar{u}_i}{\partial x_j} + \frac{\partial \bar{u}_j}{\partial x_i} \right) \quad (11)$$

#### 2.4. Combustion Model and Radiation Transport

*FDS* uses the mixture fraction model as the default combustion model [34]. The mixture fraction is a conserved scalar quantity. It is defined as the fraction of gas at a given point in the flow field that originated as fuel, as follows:

$$Z = \frac{s Y_F - (Y_{O_2} - Y_{O_2}^\infty)}{s Y_F + Y_{O_2}^\infty}; \quad s = \frac{\nu_{O_2} W_{O_2}}{\nu_F W_F}; \quad \nu_F = 1 \quad (12)$$

Where,  $Y$  is the mass fraction. Subscripts  $F$  and  $O_2$  refer to fuel and oxygen, respectively.  $Y_F^l$  is the fuel mass fraction in fuel stream. Superscript  $\infty$  refers to "far away from the fire".  $\nu$  is the stoichiometric coefficient.  $W$  is the molecular weight of gas. By design, mixture fraction varies from  $Z=1$  in a region containing only fuel to  $Z=0$  in regions (typically far away from the fire) where only ambient air with un-depleted

oxygen is present.

Radiative heat transfer is included in the model via the solution of the radiation transport equation for a non-scattering grey gas, and in some limited cases using a wide-band model. The equation is solved using a technique similar to finite-volume methods for convective transport, thus the name given to it is the Finite-Volume Method (*FVM*) [16].

## 3. Building Description and Computational Aspects

### 3.1. Building Description

The present model is a three-story building, Fig. 2, with overall plan dimensions of about  $41 \times 17 \text{ m}^2$ . The overall height is  $10 \text{ m}$ . The offices and facility are concentrated in an area of  $18 \times 13 \text{ m}^2$ . A central-rectangular hollow-section extends from the first floor to the roof of the third floor with a cross-section of  $4.4 \times 3.2 \text{ m}^2$ . The main stairs are at the right of the building. There is a stair door at each floor, Figs. 2a,f,g, with dimensions of  $2.3 \times 0.9 \text{ m}^2$ . The main door (entrance) is located at the rear of the first floor, Fig. 2h, with dimensions of  $2.7 \times 2.4 \text{ m}^2$ . Some furniture samples appear in the third floor, Figs. 2a,f.

The source of fire is a wooden disk that was altered vertically between the three floors according to the fire case, Fig. 2a.

### 3.2. Computational Mesh and Domain

The governing equations were approximated on a rectilinear mesh (grid). A computational mesh of  $202 \times 85 \times 50$  cells was used. Thus, the cells were almost cubic with dimensions of  $0.2 \times 0.2 \times 0.2 \text{ m}^3$ . Figure 3 shows some horizontal and vertical sections that illustrate the cells of the computational mesh. As can be seen, the mesh was very fine. Thus, the mesh was capable of capturing the features of both the flow and thermal fields.

As can be seen in Fig. 2, the computational domain was extended above the roof of the third floor and behind the building rear wall by about  $0.5 \text{ m}$ . These two extensions were intended to facilitate smoke exit from the upper vent (emergency opening) and the main door, respectively.

### 3.3. Boundary Conditions

Concerning the flow field, no-penetration and no-slip conditions are applied on the solid surfaces. Flow speed is determined at the openings/vents. All solid surfaces are assigned thermal boundary conditions, plus information about the burning behavior of the material. Heat and mass transfers to and from solid surfaces are handled with empirical correlations. Also, material properties of solids may be prescribed as a function of temperature [16]. For all the present building cases, the fire power was set suitable to such applications [35,47]. The normal temperature (without fire) in the building was taken as  $20^\circ\text{C}$ .

### 3.4. Investigated Cases

To investigate the effect of different possible real-life situations, fifty-seven cases were considered, table 1. These cases cover the location of fire source, the opening/closing of the stair doors and main door, and the operation of the emergency opening (vent).

The actual situation of the building has no ceiling opening (vent). The authors of the present work propose an idea to reduce fire/smoke hazards by considering an active outlet vent in the ceiling of the third floor. This emergency vent operates automatically as the fire emerges depending on the signal of heat detectors. The vent is located in the geometric center of the central-rectangular hollow-section, Fig. 4a, with dimensions of  $1.0 \times 1.0 \text{ m}^2$ . The vent opens (activates) when the temperature reaches  $40^\circ\text{C}$ . For simplicity, a heat detector was placed just above the fire source, Fig. 4b. The heat detector is moved from the ceiling of one floor to another following the fire source. The vent is equipped by a fan that may operate at three different modes, namely: (i) no operation (zero velocity), (ii) outlet velocity of  $1 \text{ m/s}$ , (iii) outlet velocity of  $5 \text{ m/s}$ .

The cases of table 1 cover the fire location at the three floors. Symbols "F", "S", and "T" refer to the location of the fire source in the first, second, and third floors, respectively. Symbol "v" refers to vent operation. In the coming sections, the stair doors will be referred as "door-1", "door-2", and "door-3" for the first, second, and third floors, respectively.

## 4. Results and Discussions

The presentation of the results considers three main times after the fire ignition, namely:  $60\text{s}$  (1 minute),  $300\text{s}$  (5 minutes), and final period. Actually,  $60\text{s}$  was chosen as a suitable time for preliminary quick evacuation of the building after fire ignition with proper alarming. Moreover,  $300\text{s}$  was considered as a suitable time for complete evacuation of the building. Final period is the time at which the smoke pattern reaches its steady (constant) shape within the building without further change with time.

### 4.1. Fire Source at the First Floor

Figure 5 shows the results of the smoke propagation for different cases. As it can be seen in Fig. 5a, after  $60\text{s}$  of fire ignition, the smoke patterns are much similar to each others with small differences. Very small amount of smoke enters the stair area due to the open stair doors, Fig. 5a(ii). The opening of the emergency vent draws the smoke from the back walking corridor near the stair area, Figs. 5a(iii), 5a(iv). Some smoke gathers in the back corridor near the closed door-3 in case F6v, Fig. 5a(iv).

Figure 5b shows the smoke patterns after  $300\text{s}$ . The smoke propagates in the three floors of the building especially the third floor for all cases without the emergency vent, Figs. 5b(i-vi). Smoke fills the stair area when door-1 is open, Fig. 5b(i). Of course, no smoke enters the stair area when all stair doors are closed, Fig. 5b(ii). The upper part of the stair area

is filled with smoke when door-3 is open, Fig. 5b(iii) while the rest of the stair area has no smoke. Small amount of smoke gathers at the upper part of the stair area when door-2 is open, Fig. 5b(iv). The stair area is partially filled with smoke when two of the stair doors are open, Figs. 5b(v,vi).

When the emergency vent is open, smoke is concentrated in the third floor, with low density in the other two floors, Figs. 5b(vii-ix). There is no smoke in the stair area when the three doors are closed, Figs. 5b(viii,ix). When the fan of the emergency vent works with full capacity ( $5 \text{ m/s}$ ), the smoke density reduces in the third floor, Fig. 5b(ix).

Figure 5c shows the smoke propagation at the final period. Table 2 shows the time in seconds of the final period for each case of Fig. 5c. The maximum period of  $1800\text{s}$  occurs when door-1 is closed (cases F8 and F12). It is clear that, by the final period, the smoke completely fills the three floors, Figs. 5c(i,ii). The upper part of the stair area is filled with smoke when door-3 is open, Figs. 5c(iii,iv). The stair area is free of smoke when the three stair doors are closed, Figs. 5c(ii,v,vi). Thus, some of the occupants can survive in the stair area until the fire fighters arrive to rescue them providing that the stair doors are well-protected against smoke leakage.

When the emergency vent is open, the smoke is drawn to the third floor, which has less smoke density comparing to other cases without the emergency vent, Figs. 5c(iv-vi). Even in the first floor, which has the fire source, the smoke is concentrated near the ceiling and thus leaving space for occupants to move with lowering their heads. When the fan of the emergency vent works with full capacity ( $5 \text{ m/s}$ ), the smoke density reduces in all floors, Fig. 5c(vi), especially the second floor which becomes almost empty of smoke. Hence, the occupants can survive in the second floor until being rescued.

As seen in Table 2, for all cases, the temperature distribution is almost the same with maximum temperature of  $170^\circ\text{C}$ , which is located in the fire area. Generally, temperature increase in the second and third floors is small. There is no temperature increase in the stair area. It is clear that the main door, whether open or closed, has a negligible effect on the smoke propagation.

### 4.2. Fire Source at the Second Floor

Figure 6 shows the results of the smoke propagation for different cases. Generally, as it can be seen in Fig. 6a, after  $60\text{s}$  of fire ignition, similar behavior to that of Fig. 5a is noticed. There are small differences between the smoke patterns. Very small amount of smoke enters the stair area due to the open stair doors, Fig. 6a(ii). The opening of the emergency vent draws the smoke from the back walking corridor near the stair area, Figs. 6a(iii,iv). Some smoke gathers in the back corridor near the closed door-3 in case S6v, Fig. 6a(iv).

Figure 6b shows the smoke patterns after  $300\text{s}$ . Mainly, the smoke propagates in the two upper floors of the building especially the third floor for all cases without the emergency vent, Figs. 6b(i-iv). Smoke fills the stair area when two or more stair doors are open, Figs. 6b(i,iv). Of course, no smoke

enters the stair area when all stair doors are closed, Fig. 6b(ii). The upper part of the stair area is filled with smoke when *door-3* is open, Fig. 6b(iii) while the rest of the stair area has no smoke.

When the emergency vent is open, smoke is concentrated in the third floor, with no smoke at all in the first floor, Figs. 6b(v-vii). Smoke gathers in the upper part of the second floor below the ceiling. Thus, occupants can move in the second floor and leave to the first floor by lowering their heads. There is no smoke in the stair area when the three doors are closed, Figs. 6b(vi,vii). When the fan of the emergency vent works with full capacity (5 m/s) and all stair doors are closed, the smoke density reduces in the third floor, Fig. 6b(vii).

Figure 6c shows the smoke propagation at the final period. Table 3 shows the time in seconds of the final period for each case of Fig. 6c. The maximum period of 1800s occurs for almost all cases, without the emergency vent working, except case *S7* (1300s) when the two doors; *door-1* and *door-3*, are open. It is clear that, by the final period, the smoke completely fills the three floors, Figs. 6c(i-v). The only exception is case *S8*, when *door-1* is closed, the smoke density in the first floor is low in the back corridor, Fig. 6c(vi). Thus, the first floor is a good resort for late evacuation when securing *door-1*. The stair area is free of smoke when the three stair doors are closed, Fig. 6c(ii).

When the emergency vent is open, the smoke is drawn to the third floor, which has less smoke density comparing to other cases without the emergency vent, Figs. 6c(vii-ix). Even in the second floor, which has the fire source, the smoke is concentrated near the ceiling and thus leaving space for occupants to move with lowering their heads. The worst case (*S6v*) happens when the three stair doors are closed, Fig. 6c(ix). Generally, it seems that the operating speed of the fan of the emergency vent has very low effect on the smoke density.

As seen in Table 3, for all cases, the temperature distribution is almost the same with maximum temperature of 170°C, which is located in the fire area. Generally, temperature increases considerably in the second floor with partial increase in the third floor. There is small temperature increase in the stair area. There is no temperature increase in the first floor. It is clear that the main door, whether open or closed, has a negligible effect on the smoke propagation.

### 4.3. Fire Source at the Third Floor

The results of this section reveal that temperature rises to very high values (around 1000°C), which leads to sudden flashover through the building. Moreover, the building structure starts to burn gradually, which may lead to a building collapse eventually. The operation of the emergency vent prevents completely this flashover. Thus, the cases are divided into two sections; one for flashover and the other for operation of the emergency vent.

#### 4.3.1. Cases of Flashover

Whether or not "flashover" occurs during the course of a fire is one of the most important outcomes of a fire

calculation. Flashover is characterized by the rapid transition to fire behavior from localized burning source to the involvement of all combustibles in the enclosure. High radiation heat transfer levels from the original burning item, the flame and plume directly above it, and the hot smoke layer spreading across the ceiling are all considered to be responsible for the heating of the other items, leading to their ignition. Factors affecting flashover include enclosure size, ceiling and wall conductivity and flammability, and heat- and smoke-producing quality of enclosure contents [48].

In the present study, warning signs of flashover were noticed just before the actual occurrence of flashover. These signs include heat build-up and "rollover". Rollover means small, sporadic flashes of flame that appear near ceiling level or at the top open doorways of smoke-filled enclosures [48].

This section covers all the investigated cases (*T1-T13*) without the operation of the emergency vent. Figure 7 shows the smoke propagation due to the fire source in the third floor. After 60s, the smoke pattern is exactly the same for all cases, Fig. 7a. Smoke is concentrated in the upper portion of the third floor, while the other two floors are completely free of smoke. Just before flashover, Fig. 7b, the smoke completely fills the third floor. When the three stair doors are open or *door-1* and *door-3* are open, smoke fills completely the stair area and sneaks partially to the first and second floors, Fig. 7b(i). When the three stair doors are closed or only one door is open, smoke fills completely the third floor, and partially the second floor, whereas the first floor is approximately free of smoke, Fig. 7b(ii). When *door-3* is open, smoke partially fills the upper half of the stair area and the second floor, Fig. 7b(iii). It is noticed that, in all cases, the first floor is completely or partially free of smoke, which represents good resort for occupants to get out of the building through the main door.

Figure 7c shows the smoke propagation at time of flashover for all cases (*T1-T13*). Both smoke and fire propagate in the whole building. Figure 7d shows the smoke propagation after time of flashover without structure burning for many cases. It is clear thus fire is decaying. Figure 7e illustrates the smoke propagation after time of structure burning for some cases (*T4, T6, T7, T10, T13*). Some parts of the structure are vanished due to flashover and high temperature rise. As can be seen in table 4, when the structure starts to burn, the maximum temperature is constant at 1000°C. It is clear from table 4 that the time of flashover is case-dependent and the maximum temperature is around 1000°C.

Figure 8 demonstrates the temperature distribution in cases of flashover. It is clear that sudden temperature rise occurs at the time of flashover in the whole building, Fig. 8b. However, in cases of structure burning, the temperature lowers after its sudden rise, Fig. 8c.

Figure 9 shows the development of the structure burning with time for case *T6* as an example.

#### 4.3.2. Cases of Operation of Emergency Vent

For all cases of operation of emergency vent (*T1v-T6v*),

there is no flashover and structure burning. Figure 10 illustrates the patterns of smoke propagation with operation of the emergency vents (without flashover). After 60s, the smoke pattern is the same for all cases, Fig. 10a. Smoke is concentrated in the upper portion of the central area of the third floor. Smoke is sucked out the building through the emergency vent.

After 300s, the same pattern is kept as that after of 60s when the fan of the emergency vent operates at full capacity (5 m/s) with the three stair doors are open, Fig. 10b(ii). In other cases, Figs. 10(i,iii,iv), the smoke propagates in other parts of the third floor but restricted to the upper portion. The two other floors are completely free of smoke.

After 1800s (the final period), the minimum density of the smoke is noticed when the fan of the emergency vent operates at full capacity (5 m/s), Figs. 10c(ii,v). Maximum smoke density is seen in the case (T2v) of the closed stair doors and the emergency vent is open with no fan working (0 m/s), Fig. 10c(iii). In all cases, Fig. 10c(i-v), the first and second floors as well as the stair area are completely free of smoke.

Fig. 11 demonstrates the temperature distribution in all the six cases. It is obvious that the operation of the emergency vent reduces the maximum temperature to 170°C which is much less and safer in comparison to the cases without

emergency vent when maximum temperatures becomes about 1000°C, table 4.

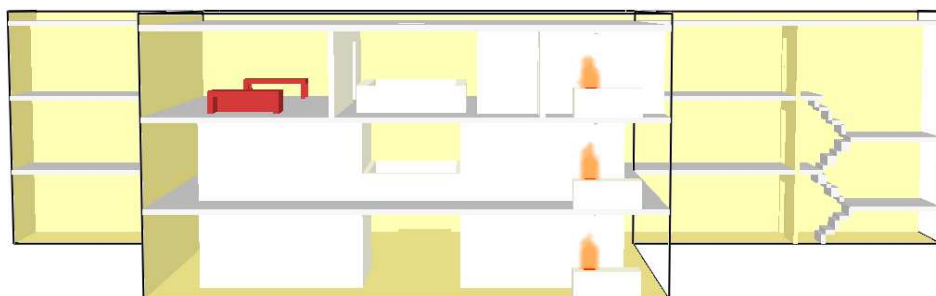
#### 4.4. Smoke Exit of the Main Door

The smoke exit of the main door is an important factor in the evacuation plans. Table 5 illustrates the time at which the smoke starts to exit from the main door for all cases. As can be seen in table 5, the time of smoke exit, from the main door, increases considerably when the fire source moves from the first floor to the third floor. Considering the fire source in the first floor, the operation of the emergency vent approximately doubles the time required for the smoke to start exiting from the main door. However, for the fire source in the second or third floors, the operation of the emergency vent prevents completely the exit of smoke from the main door. Thus, the operation of the emergency vent helps greatly in the evacuation of the occupants from the main door of the building.

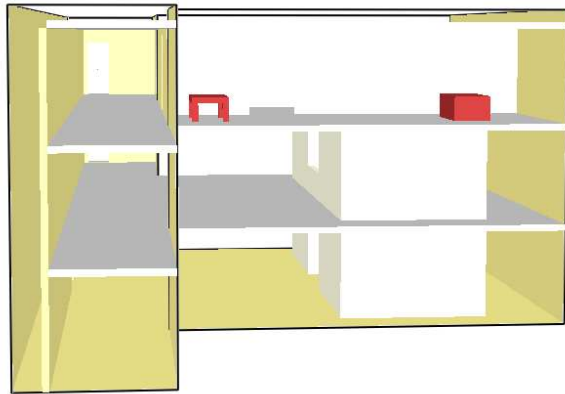
Figure 12 shows the progress of smoke exit of the main door with time of case F1 as an example. The smoke exiting from the main door is restricted to the upper portion of the main door till 180s (3 minutes). Thus, occupants can easily and safely leave the main door.



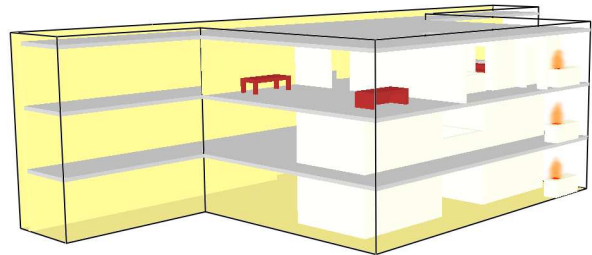
Fig. 1. Typical hot-smoke test layout using smoke canister [15].



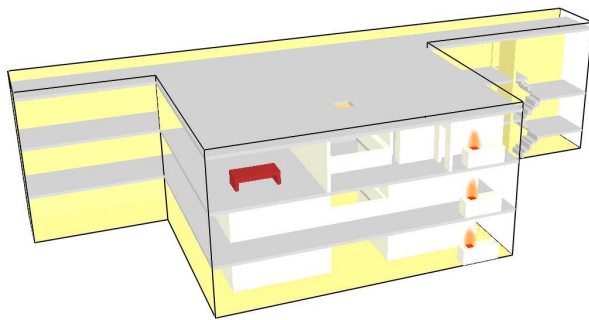
(a) Front view.



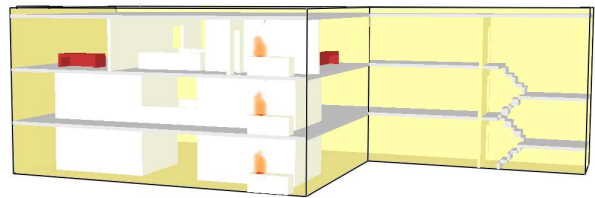
(b) Side view.



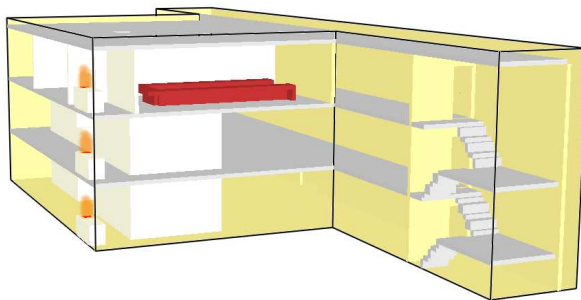
(c) Inclined view.



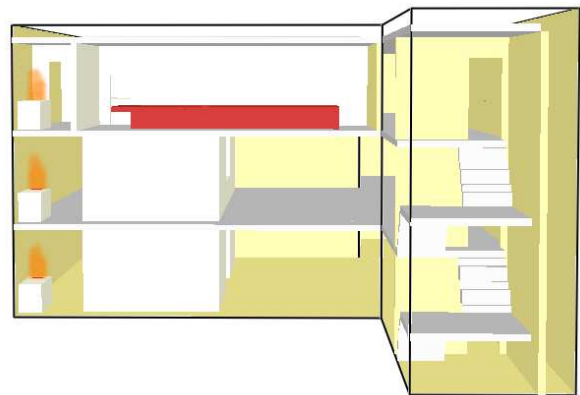
(d) Inclined view.



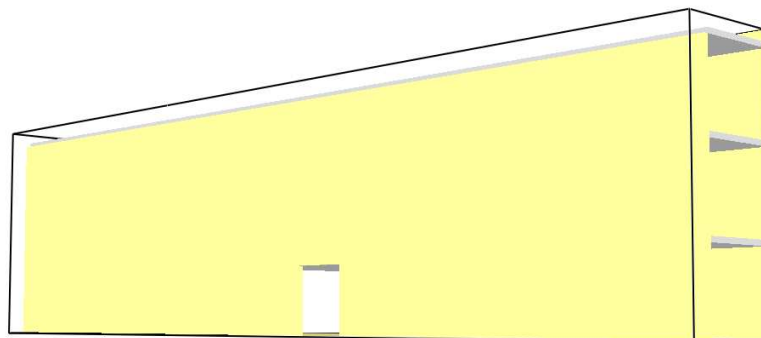
(e) Inclined view.



(f) Inclined view.



(g) Side view.



(h) Rear view.

**Fig. 2.** Views showing the details of the three floors of the building.

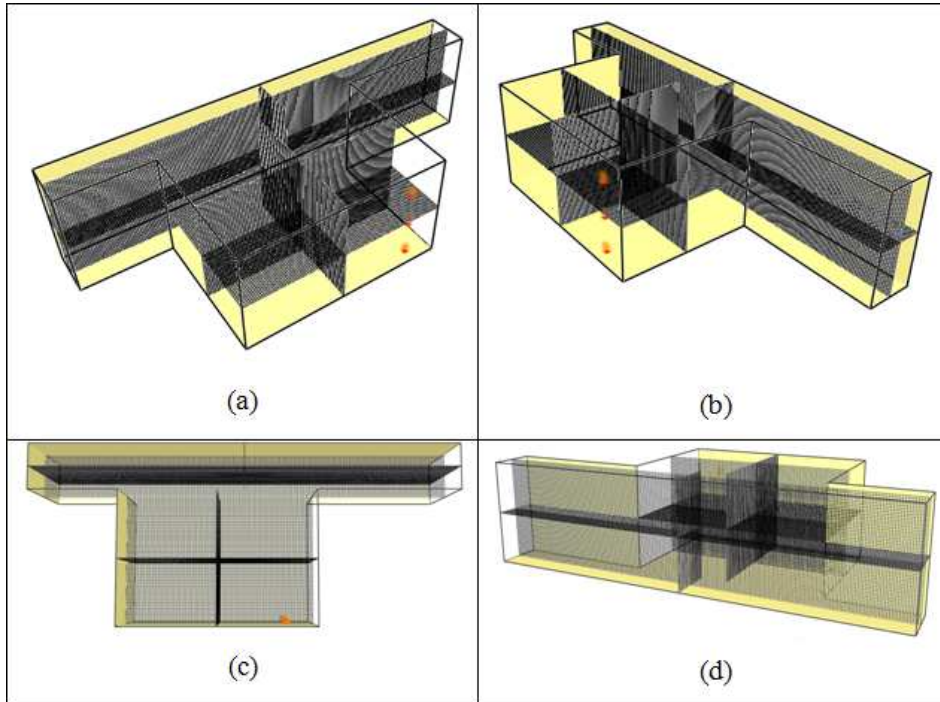
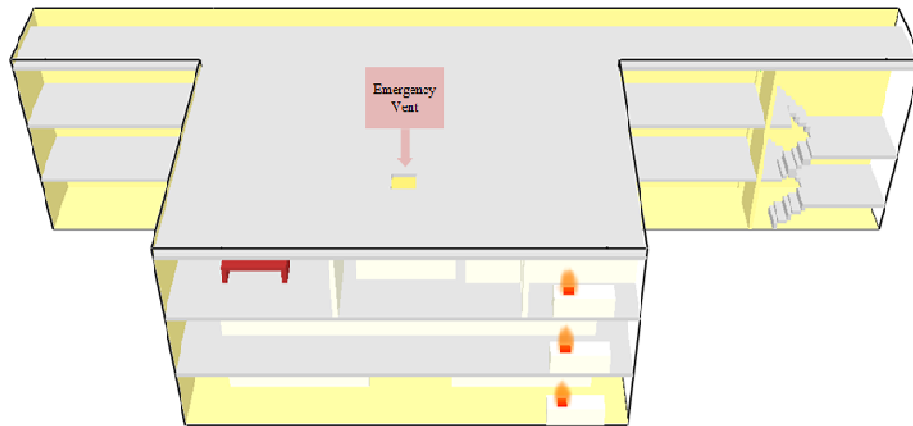
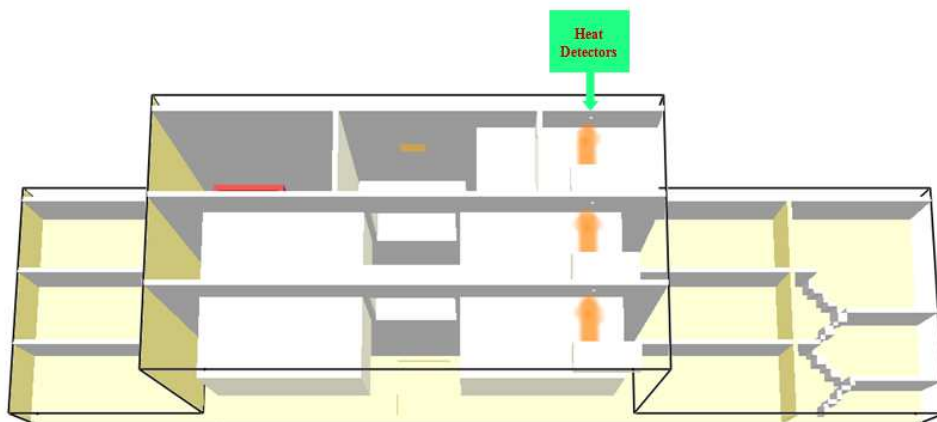


Fig. 3. Views of the elements (cells) of the computational mesh.



(a) Top view showing the location of the proposed opening (emergency vent).

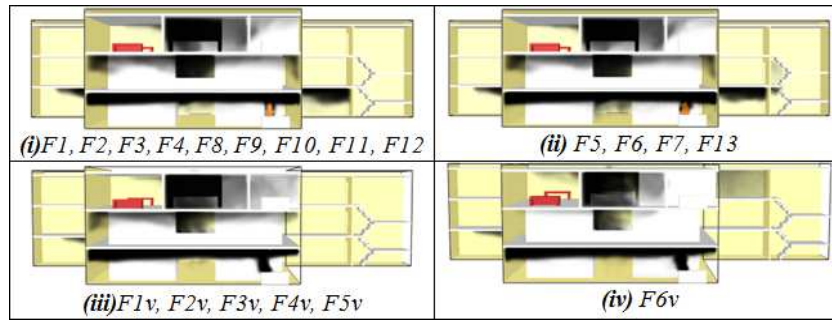


(b) Locations of the three heat detectors.

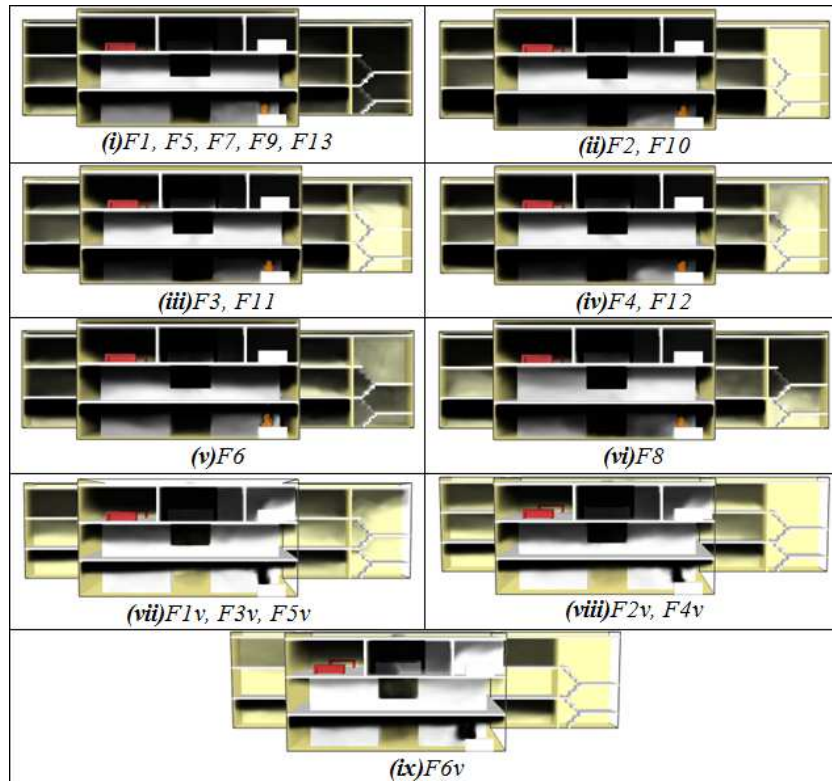
Fig. 4. Views of the smoke detectors and emergency vent.

Table 1. Cases of the present study.

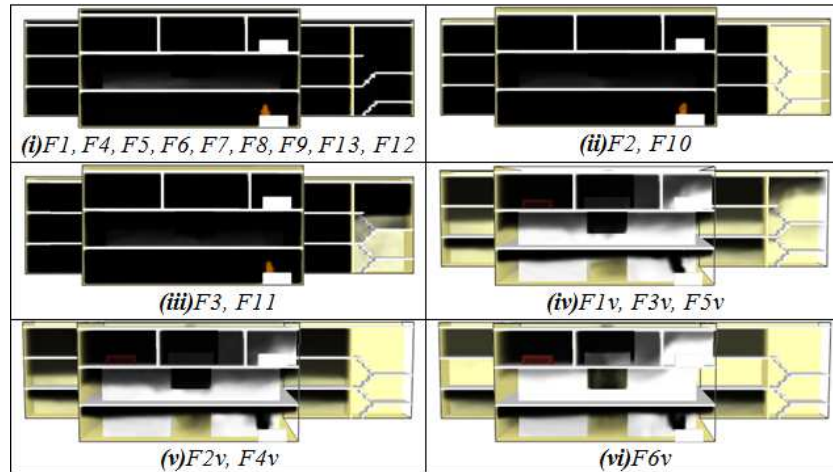
No.	First Floor Cases	Second Floor Cases	Third Floor Cases	Main door	First floor stair door	Second floor stair door	Third floor stair door	Emergency vent
1	F1	S1	T1	Open	Open	Open	Open	Closed
2	F2	S2	T2	Open	Closed	Closed	Closed	Closed
3	F3	S3	T3	Open	Closed	Closed	Open	Closed
4	F4	S4	T4	Open	Closed	Open	Closed	Closed
5	F5	S5	T5	Open	Open	Closed	Closed	Closed
6	F6	S6	T6	Open	Open	Open	Closed	Closed
7	F7	S7	T7	Open	Open	Closed	Open	Closed
8	F8	S8	T8	Open	Closed	Open	Open	Closed
9	F9	S9	T9	Closed	Open	Open	Open	Closed
10	F10	S10	T10	Closed	Closed	Closed	Closed	Closed
11	F11	S11	T11	Closed	Closed	Closed	Open	Closed
12	F12	S12	T12	Closed	Closed	Open	Closed	Closed
13	F13	S13	T13	Closed	Open	Closed	Closed	Closed
14	F1v	S1v	T1v	Open	Open	Open	Open	Open (0 m/s)
15	F2v	S2v	T2v	Open	Closed	Closed	Closed	Open (0 m/s)
16	F3v	S3v	T3v	Open	Open	Open	Open	Open (1 m/s)
17	F4v	S4v	T4v	Open	Closed	Closed	Closed	Open (1 m/s)
18	F5v	S5v	T5v	Open	Open	Open	Open	Open (5 m/s)
19	F6v	S6v	T6v	Open	Closed	Closed	Closed	Open (5 m/s)



a. Smoke propagation after 60s.



b. Smoke propagation after 300s.

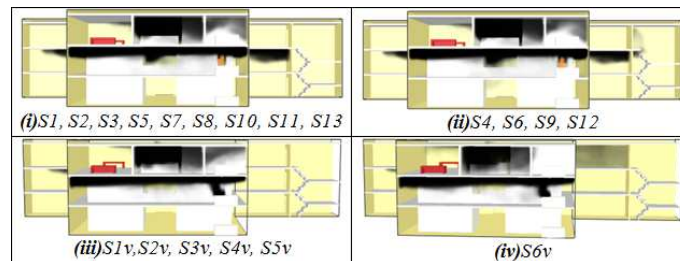


c. Smoke propagation at final period.

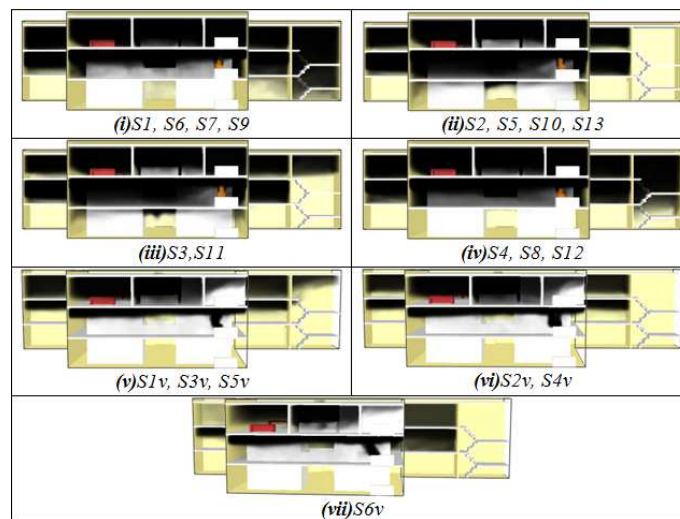
Fig. 5. Views of the smoke propagation due to fire source in the first floor.

Table 2. Final period and maximum temperature due to fire source in the first floor for different cases.

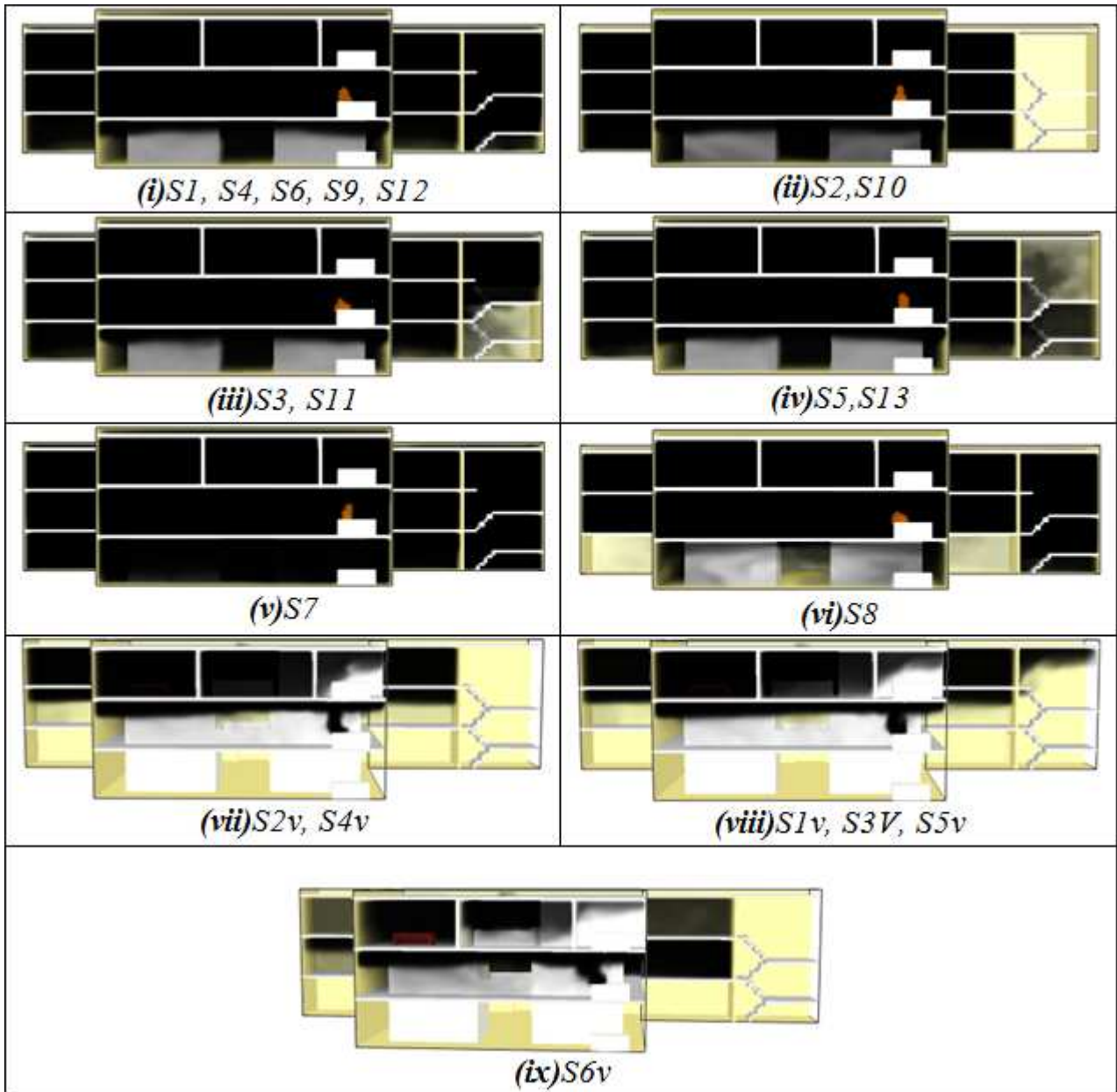
Case	Final time	Maximum Temperature = 170°C
F7, F9, F13	900s	
F10, F11	1000s	
F1, F3, F5, F6, F2, F4, F1v, F3v, F5v, F2v, F4v, F6v	1200s	
F8, F12	1800s	



a. Smoke propagation after 60s.



b. Smoke propagation after 300s.

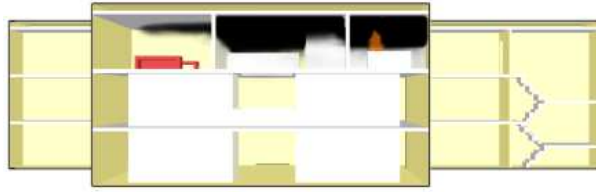


c. Smoke propagation at final period.

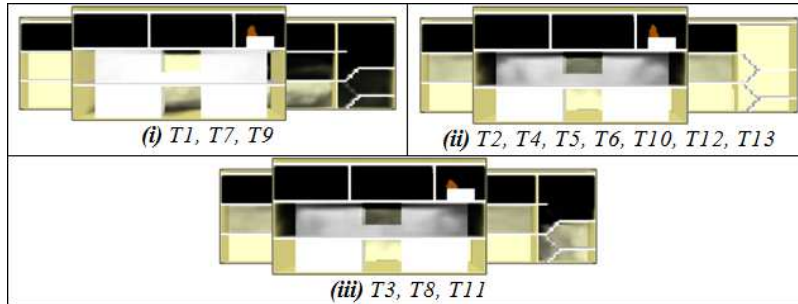
Fig. 6. Views of the smoke propagation due to fire source in the second floor.

Table 3. Final period and maximum temperature due to fire source in the second floor for different cases.

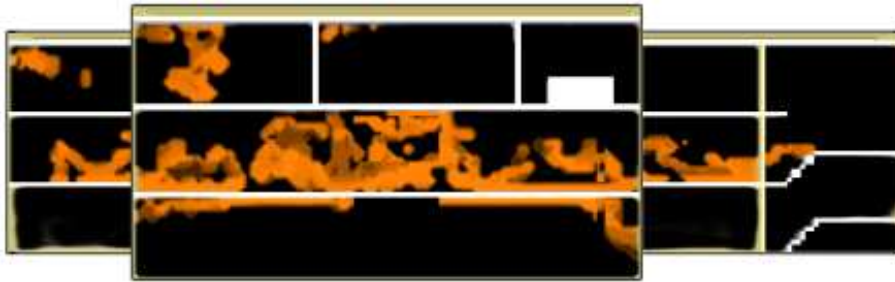
Case	Final time	Maximum Temperature = 170°C
S1v, S3V, S5v, S2v, S4v, S6v	1200s	
S7	1300s	
S1, S4, S6, S9, S12, S2,S10, S3, S11, S5,S13, S8	1800s	



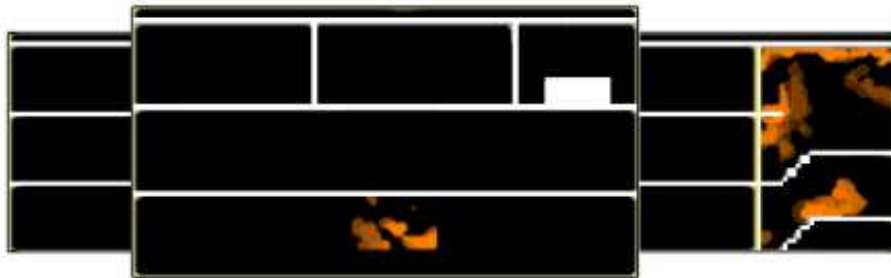
*T1, T2, T3, T4, T5, T6, T7, T8, T9, T10, T11, T12, T13*  
 a. Smoke propagation after 60s.



b. Smoke propagation before flashover.



*T1, T2, T3, T4, T5, T6, T7, T8, T9, T10, T11, T12, T13*  
 c. Smoke propagation at time of flashover.



*T1, T2, T3, T5, T8, T9, T11, T12*  
 d. Smoke propagation after time of flashover without structure burning.

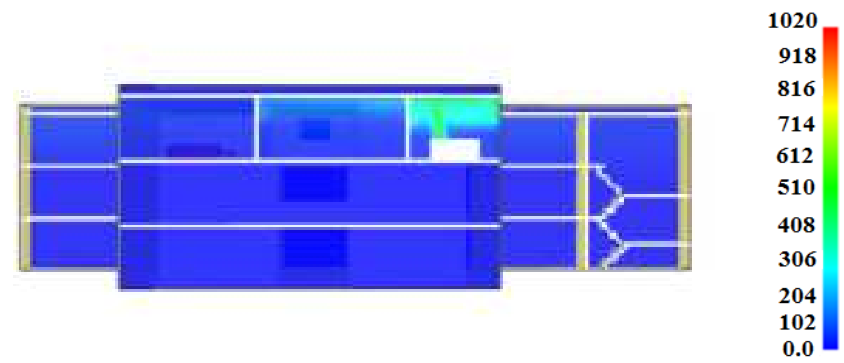


*T4, T6, T7, T10, T13*  
 e. Smoke propagation after time of structure burning.

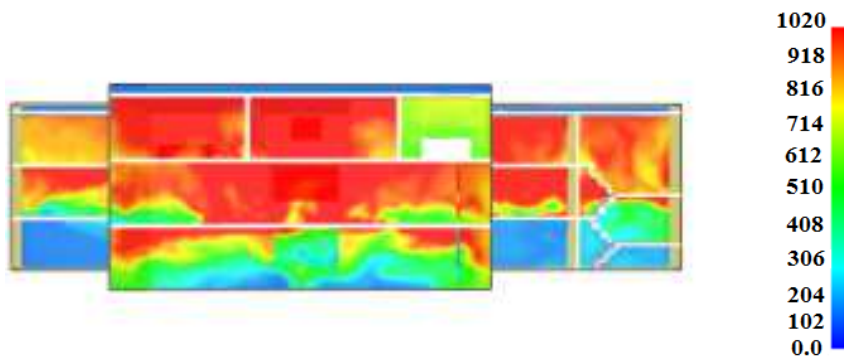
**Fig. 7. Views of the smoke propagation due to fire source in the third floor.**

**Table 4.** Time of flashover and maximum temperature.

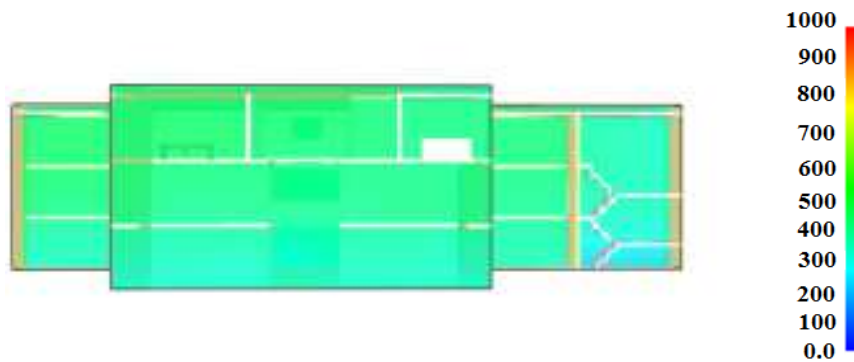
Case	Time of flashover (s)	Max. Temperature (°C)
T1	1365	1020
T2	1255	970
T3	1348	1020
T4	1280	1000
T5	1274	1020
T6	1253	1000
T7	1370	1000
T8	1384	970
T9	1387	1020
T10	1267	1000
T11	1357	970
T12	1264	1020
T13	1255	1000



T1-T13  
a. Before flashover.

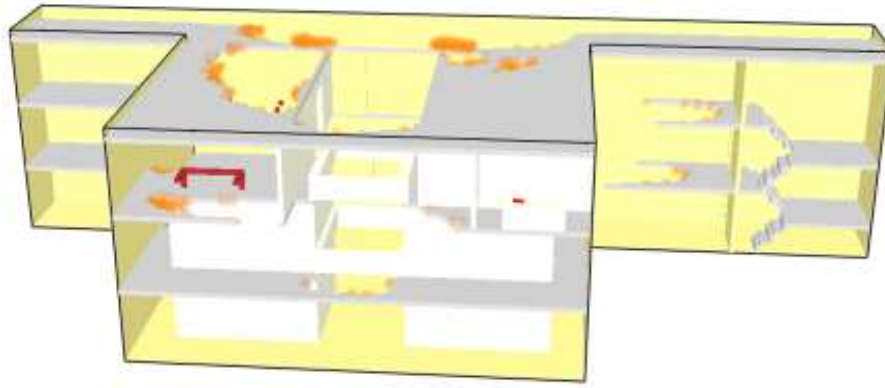


T1-T13  
b. At time of flashover.

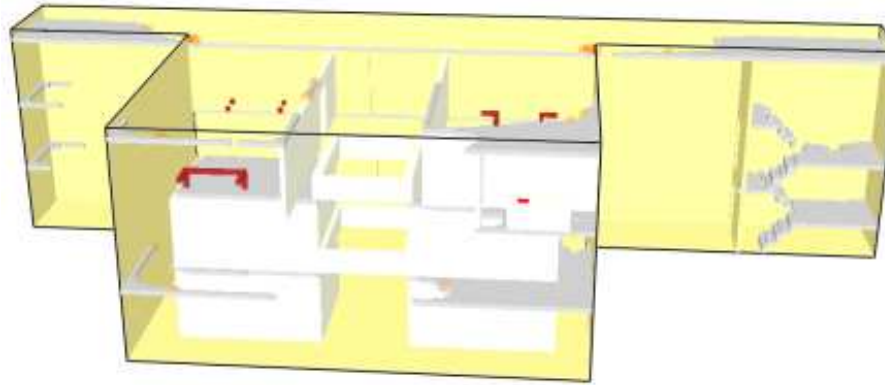


T4, T6, T7, T10, T13  
c. After structure burning.

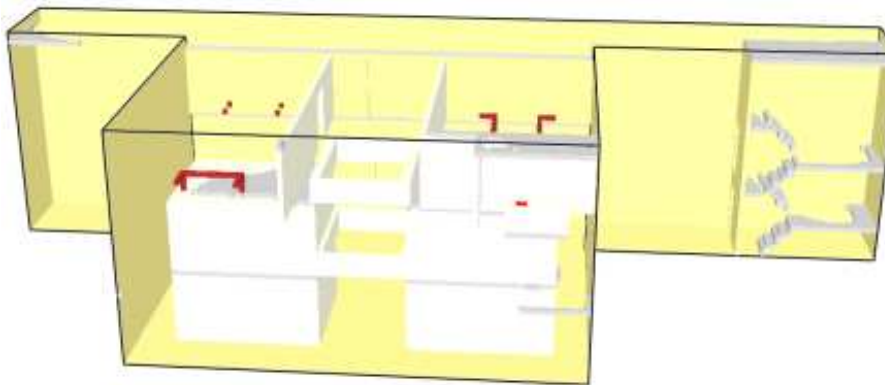
**Fig. 8.** Temperature distribution due to fire source in the third floor in cases of flashover.



(a) Time = 1332s



(b) Time = 1400s

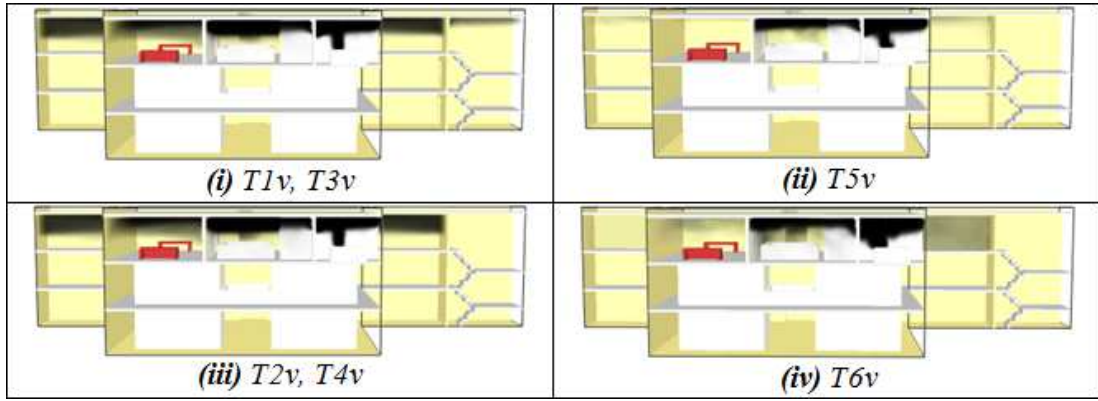


(c) Time = 1800s

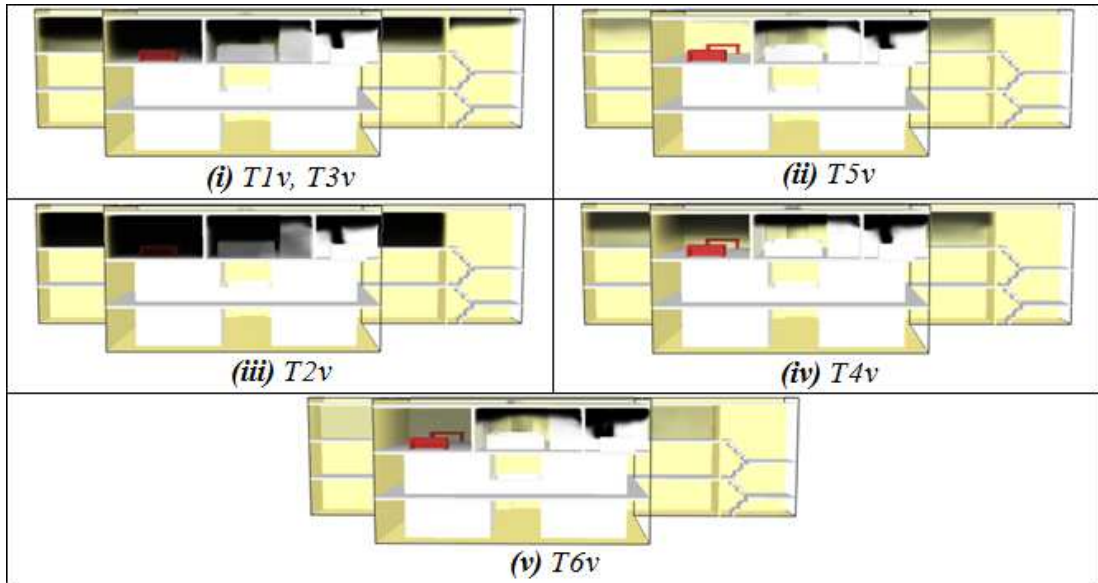
**Fig. 9.** Views of the structure burning due to fire source in the third floor at different time periods (Case T6 as an example).



*T1v, T2v, T3v, T4v, T5v, T6v*  
a. Smoke propagation after 60s.

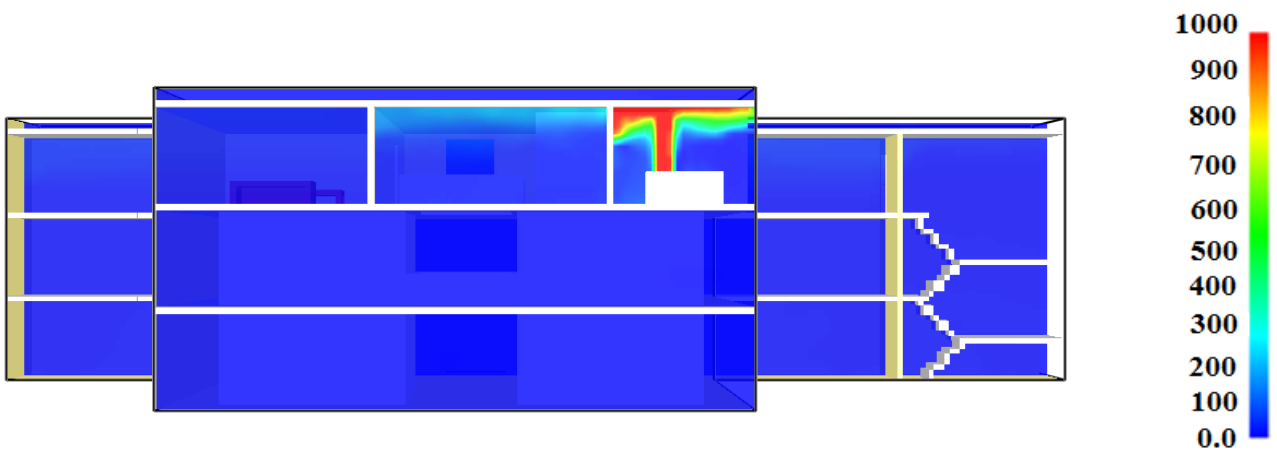


b. Smoke propagation after 300s.



c. Smoke propagation at final period (1800s).

Fig. 10. Views of the smoke propagation due to fire source in the third floor without flashover (operation of emergency vent).



$T1v, T2v, T3v, T4v, T5v, T6v$  (Max Temperature =  $170^{\circ}\text{C}$ )

Fig. 11. Temperature distribution due to fire source in the third floor without flashover.

Table 5. Time of smoke exit out of the main door.

First floor cases	Time (s)	Second floor cases	Time (s)	Third floor cases	Time (s)
F1	30	S1	240	T1	1125
F2	30	S2	270	T2	1250
F3	30	S3	220	T3	1345
F4	30	S4	220	T4	1272
F5	30	S5	215	T5	1268
F6	30	S6	485	T6	1247
F7	30	S7	230	T7	1357
F8	30	S8	675	T8	1382
F9	Closed	S9	Closed	T9	Closed
F10	Closed	S10	Closed	T10	Closed
F11	Closed	S11	Closed	T11	Closed
F12	Closed	S12	Closed	T12	Closed
F13	Closed	S13	Closed	T13	Closed
F1v	60	S1v	No exit	T1v	No exit
F2v	60	S2v	No exit	T2v	No exit
F3v	57	S3v	No exit	T3v	No exit
F4v	57	S4v	No exit	T4v	No exit
F5v	57	S5v	No exit	T5v	No exit
F6v	57	S6v	No exit	T6v	No exit

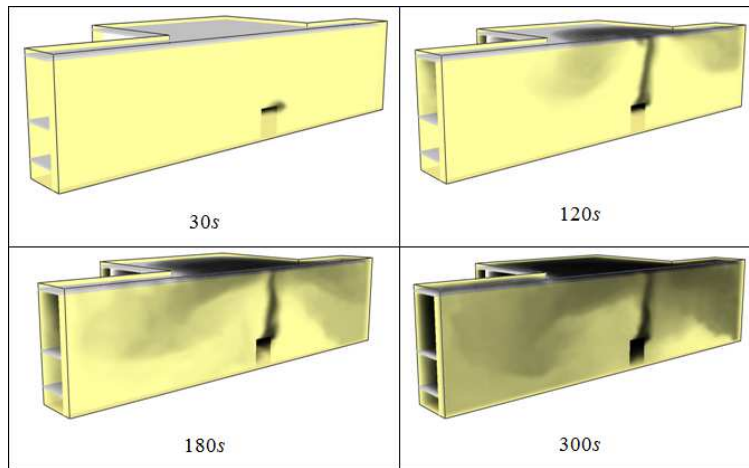


Fig. 12. Progress of smoke exit of the main door with time (Case F1 as an example).

### 5. Conclusions

Based on the above results and discussions, the following concluding points can be stated:

- (i) Temperature may rise to unexpected very high levels and flashover occurs when the smoke does not find its way out of the building. This is typically happened in the present study for the cases of fire source in the third floor. Depending on the material of the structure, this may lead to structure burning and/or building collapse.
- (ii) Distribution of temperature and its maximum value are dependent on the fire location and the outlet openings of the smoke.
- (iii) Emergency vents in the roof of the top floor, which operate in time of fire based on the signal of heat/smoke detectors, play an outstanding job in sucking the smoke outside the building. Thus, flashover is prevented and evacuation of the occupants becomes much easier and safer.
- (iv) In some of the investigated cases, the emergency

- vents may cause the first and/or the second floors to be fully or partially free of smoke for a relatively large period of time (20 or 30 minutes).
- (v) Naturally, the increase of the speed of the fan of the emergency vent draws more smoke out of the building. However, in certain cases, just the vent opening without fan operation helps greatly in sucking the smoke out of the building.
- (vi) The location of the fire source, relative to the building floors, affects significantly the smoke propagation and density.
- (vii) The inner openings between different floors facilitate the smoke propagation from one floor to another. This situation is very tricky to the occupants and may cause serious injuries.
- (viii) The condition of the stair doors; open or closed, has an important effect on the smoke propagation. Smoke may move from the upper floor to a lower floor through the open doors of the stair area.
- (ix) In certain cases, the stair area may be fully or partially free of smoke for a considerably long period

of time. Thus, the stair area becomes a good resort for occupants until the arrival of fire fighters to rescue them providing that the stair doors are well-insulated against smoke leakage.

- (x) Generally, the condition of the main door; open or closed, has a little effect on the smoke propagation. However, it is essential to study the smoke movement out of it for proper evacuation plans.
- (xi) Occupants should be trained to obey the emergency and evacuation plans especially lowering their heads below the smoke layer to survive. In many of the investigated cases, the smoke is constrained to the upper portion of the floor just below the ceiling.

## Acknowledgement

The authors would like to acknowledge Engs. B. S. Qattan, O. S. Yamani, H. H. Bahha, S. A. Gubali, B. A. Al-Sobhi, and N. M. Al-Harbi for their efforts to complete the present study.

## Nomenclature

$C_s$	= modeling constant.
$F$	= summation of external forces.
$H$	= enthalpy.
$Q$	= heat transfer.
$\dot{q}'''$	= heat release rate per unit volume ( <i>HRRPUV</i> ).
$P$	= pressure.
$\bar{p}$	= filtered pressure field.
$\bar{S}_{ij}$	= magnitude of the large-scale strain rate tensor.
$T$	= temperature.
$u_i$	= velocity in $i$ -direction, $i=1, 2, 3$ .
$u_i u_j$	= nonlinear filtered advection term.
$W$	= molecular weight of gas.
$Y$	= mass fraction.
$Y_F^l$	= fuel mass fraction in fuel stream.
$Z$	= mixture fraction.

## Greek

$\delta_{ij}$	= Kronecker's delta.
$\Delta_g$	= filter width.
$\Delta_x, \Delta_y$ and $\Delta_z$	= grid sizes in the Cartesian coordinates $x, y$ and $z$ , respectively.
$\Phi$	= any heat source.
$\nu$	= stoichiometric coefficient.
$\nu_T$	= Turbulent eddy viscosity.
$\rho$	= fluid density.
$\tau_{ij}$	= subgrid-scale stress tensor.

## Superscripts and Subscripts

$\infty$	= refers to "far away from the fire".
$F$	= refers to "fuel".
$O_2$	= refers to "oxygen".

## Abbreviations

<i>ASTM</i>	= American Society for Testing and Materials.
<i>BFST</i>	= Bureau of Fire Standards and Training.
<i>CFD</i>	= Computational Fluid Dynamics.
<i>DNS</i>	= Direct Numerical Simulation.
<i>FDS</i>	= Fire Dynamic Simulator.
<i>FPA</i>	= Fire Protection Association Australia.
<i>FVM</i>	= Finite-Volume Method.
<i>HRRPUV</i>	= Heat Release Rate per Unit Volume.
<i>LES</i>	= Large Eddy Simulation.
<i>NFPA</i>	= National Fire Protection Association.
<i>NIST</i>	= National Institute of Standards and Technologies.
<i>RANS</i>	= Reynolds-Averaged Navier-Stokes.
<i>SBI</i>	= Single Burning Item.
<i>SGS</i>	= Sub-Grid Scale.

## References

- [1] W. Men, K. B. McGrattan, and H. R. Baum, "Large Eddy Simulations of Fire-Driven Flows", *ASME National Heat Transfer Conference*, Vol. 2, 1995.
- [2] A. Kashef, N. Bénichou, G. Lougheed, and A. Debs, "Computational Fluid Dynamics Simulations of in-Situ Fire Tests in Road Tunnels", *5th International Conference-Tunnels Fires*, London, UK, pp. 185-196, Oct. 25-27, 2004.
- [3] Y. Xin, J. P. Gore, K. B. McGrattan, R. G. Rehm, and H. R. Baum, "Fire Dynamics Simulation of a Turbulent Buoyant Flame Using a Mixture-Fraction-Based Combustion Model", *Combustion and Flame J.*, Vol. 141, pp. 329-335, 2005.
- [4] W. Jahn, G. Rein, and J. L. Torero, "The Effect of Model Parameters on the Simulation of Fire Dynamics", *Fire Safety Science*, Vol. 9, pp. 1341-1352, 2008.
- [5] Y. Huo, Y. Gao, and W. Chow, "Locations of Diffusers on Air Flow Field in an Office," *The Seventh Asia-Pacific Conference on Wind Engineering*, Taipei, Taiwan, November 8-12, 2009.
- [6] L. Razdolsky, "Mathematical Modeling of Fire Dynamics," *Proceedings of the World Congress on Engineering 2009*, London, U.K., Vol. II, July 1 - 3, 2009.
- [7] H. Cheng, and G. V. Hadjisophocleous, "Dynamic Modeling of Fire Spread in Building", *Fire Safety Journal*, Vol. 46, No. 4, pp. 211-224, 2011.
- [8] D. Ling, and K. Kan, "Numerical Simulations on Fire and Analysis of the Spread Characteristics of Smoke in Supermarket", In *Advanced Research on Computer Education, Simulation and Modeling*, pp. 7-13, Springer Berlin Heidelberg, 2011.
- [9] P. Yang, X. Tan, and W. Xin, "Experimental Study and Numerical Simulation for a Storehouse Fire Accident", *Building and Environment*, Vol. 46, No. 7, pp. 1445-1459, 2011.
- [10] C. Zhang, and G. Q. Li, "Fire Dynamic Simulation on Thermal Actions in Localized Fires in Large Enclosure", *Advanced Steel Construction*, Vol. 8, pp. 124-136, 2012.

- [11] R. Sun, Z. Huang, and I. W. Burgess, "Progressive Collapse Analysis of Steel Structures under Fire Conditions", *Engineering Structures*, Vol. 34, pp. 400-413, 2012.
- [12] A. H. Wu, and L. C. Chen, "3D Spatial Information for Fire-fighting Search and Rescue Route Analysis within Buildings", *Fire Safety Journal*, Vol. 48, pp. 21-29, 2012.
- [13] A. Agarwal, and A. H. Varma, "Fire Induced Progressive Collapse of Steel Building Structures: The Role of Interior Gravity Columns", *Engineering Structures*, Vol. 58, pp. 129-140, 2014.
- [14] M. He, and Y. Jiang, "Use *FDS* to Assess Effectiveness of Air Sampling-Type Detector for Large Open Spaces Protection", *Vision Fire & Security*, 2005.
- [15] A. Webb, "*FDS* Modelling of Hot Smoke Testing, Cinema and Airport Concourse", Thesis of Master of Science, The Faculty of the Worcester Polytechnic Institute, USA, 2006.
- [16] P. Smardz, "Validation of Fire Dynamics Simulator (*FDS*) for Forced and Natural Convection Flows", Master of Science in Fire Safety Engineering, University of Ulster, 2006.
- [17] R. Sun, M. A. Jenkins, S. K. Krueger, W. Mell, and J. J. Charney, "An Evaluation of Fire-Plume Properties Simulated with the Fire Dynamics Simulator (*FDS*) and the Clark Coupled Wildfire Model," *Can. J. for Res.*, Vol. 36, pp. 2894-2908, 2006.
- [18] P. Coyle, and V. Novozhilov, "Further Validation of Fire Dynamics Simulator Using Smoke Management Studies", *International Journal on Engineering Performance-Based Fire Codes*, Vol. 9, No. 1, pp.7-30, 2007.
- [19] J. Zhang, M. Delichatsios, and M. Colobert, "Assessment of Fire Dynamics Simulator for Heat Flux and Flame Heights Predictions from Fires in *SBI* Tests", *Fire Technology*, Vol. 46, pp. 291-306, 2010.
- [20] N. Wu, R. Yang, and H. Zhang, "A Distributed Method for Predicting Building Fires Based on a Two-Layer Zone Model", *ASME 2013 International Mechanical Engineering Congress and Exposition*, 2013.
- [21] X. T. Zhang, and S. L. Wang, "Numerical Simulation of Smoke Movement in Vertical Shafts during a High-Rise Building Fire", *Applied Mechanics and Materials*, Vol. 438, pp. 1824-1829, 2013.
- [22] Y. Jiang, G. Rein, S. Welch, and A. Usmani, "Modeling Fire-Induced Radiative Heat Transfer in Smoke-Filled Structural Cavities", *International Journal of Thermal Sciences*, Vol. 66, pp. 24-33, 2013.
- [23] Y. Yu, Y. Y. Chu, and D. Liang, "Study on Smoke Control Strategy in a High-rise Building Fire", *Procedia Engineering*, Vol. 71, pp. 145-152, 2014.
- [24] X. Zhang, S. Wang, and J. Wang, "Numerical Simulation of Smoke Movement in Vertical Shafts during High-Rise Fires Using a Modified Network Model", *Journal of Chemical & Pharmaceutical Research*, Vol. 6, No. 6, 2014.
- [25] S. Bae, H. J. Shin, and H. S. Ryou, "Development of CAU\_USCOP, A Network-Based Unsteady Smoke Simulation Program for High-Rise Buildings. *Building Simulation*, Vol. 7, No. 5, pp. 503-510, 2014.
- [26] F. Tingyong, X. Jun, Y. Jufen, and W. Bangben, "Study of Building Fire Evacuation Based on Continuous Model of *FDS* & *EVAC*", In *Computer Distributed Control and Intelligent Environmental Monitoring (CDCIEM)*, IEEE Conference, pp. 1331-1334, 2011.
- [27] F. Tang, and A. Ren, "GIS-based 3D evacuation simulation for indoor fire", *Building and Environment*, Vol. 49, pp. 193-202, 2012.
- [28] L. Zhang, Y. Wang, H. Shi, and L. Zhang, "Modeling and analyzing 3D complex building interiors for effective evacuation simulations", *Fire Safety Journal*, Vol. 53, pp. 1-12, 2012.
- [29] <http://www.fire.nist.gov/fds/>, <http://www.nist.gov/index.html>
- [30] A. F. Abdel-Gawad, and H. A. Ghulman, "Fire Dynamics Simulation of Large Multi-story Buildings, Case Study: Umm Al-Qura University Campus", *International Conference on Energy and Environment 2013 (ICEE2013)*, Universiti Tenaga Nasional, Putrajaya Campus, Selangor, Malaysia, 5-6 March 2013. [Institute of Physics (IOP) Conference Series: Earth and Environmental Science, Vol. 16, issue 1, 2013, doi:10.1088/1755-1315/16/1/012040].
- [31] G. P. Forney, *Smokeyview (Version 5)-A Tool for Visualizing Fire Dynamics Simulation Data - Volume I: User's Guide*, *NIST Special Publication 1017-1*, 2010.
- [32] G. P. Forney, *Smokeyview (Version 5)-A Tool for Visualizing Fire Dynamics Simulation Data - Volume II: Technical Reference Guide*, *NIST Special Publication 1017-2*, 2010.
- [33] G. P. Forney, *Smokeyview (Version 5)-A Tool for Visualizing Fire Dynamics Simulation Data - Volume III: Verification Guide*, *NIST Special Publication 1017-3*, 2010.
- [34] K. McGrattan, S. Hostikka, J. Floyd, H. Baum, R. Rehm, W. Mell, and R. McDermott, *Fire Dynamics Simulator (Version 5)-Technical Reference Guide-Volume 1: Mathematical Model*, *NIST Special Publication 1018-5*, 2010.
- [35] K. McGrattan, R. McDermott, S. Hostikka, and J. Floyd, *Fire Dynamics Simulator (Version 5)-User's Guide*, *NIST Special Publication 1019-5*, 2010.
- [36] K. McGrattan, S. Hostikka, J. Floyd, and B. Klein, *Fire Dynamics Simulator (Version 5) Technical Reference Guide - Volume 3: Validation*, *NIST Special Publication 1018-5*, 2010.
- [37] National Fire Protection Association (NFPA): The American authority on fire, electrical, and building safety: <http://www.nfpa.org>
- [38] British Standards: <http://shop.bsigroup.com>
- [39] The Bureau of Fire Standards and Training (*BFST*), Division of State Fire Marshal, Florida, USA: [http://www.myfloridacfo.com/sfm/bfst/bfst\\_index.htm](http://www.myfloridacfo.com/sfm/bfst/bfst_index.htm)
- [40] Fire Protection Association Australia (FPA), Australia: <http://www.fpaa.com.au>
- [41] *ASTM* International, formerly known as the American Society for Testing and Materials (*ASTM*), USA: <http://www.astm.org/Standards/fire-and-flammability-standards.html>
- [42] Alaska Fire Standards Council, Alaska, USA <http://dps.alaska.gov/AFSC/>

- [43] Fire Commissioner of Canada Standards: [http://www.hrsdc.gc.ca/eng/labour/fire\\_protection/policies\\_standards](http://www.hrsdc.gc.ca/eng/labour/fire_protection/policies_standards)
- [44] A. Leonard, "Energy Cascade in Large-Eddy Simulations of Turbulent Fluid Flows", *Advances in Geophysics A*, Vol. 18, pp. 237–248, 1974.
- [45] J. Smagorinsky, "General Circulation Experiments with the Primitive Equations", *Monthly Weather Review*, Vol. 91 (3), pp. 99–164, 1963.
- [46] J. Deardorff, "A Numerical Study of Three-Dimensional Turbulent Channel Flow at Large Reynolds Numbers", *Journal of Fluid Mechanics*, Vol. 41 (2), pp. 453–480, 1970.
- [47] Z.-C. Grigoraş, and D. Diaconu-Şotropa, "Establishing the Design Fire Parameters for Buildings", *Bul. Inst. Polit. Iaşi*, t. LIX (LXIII), f. 5, pp. 133-141, 2013.
- [48] H.-J. Kim, and D. G. Lilley, "Heat Release Rates of Burning Items in Fires", 38<sup>th</sup> Aerospace Sciences Meeting & Exhibit, Reno, Nevada, USA, 10-13 January 2000, AIAA 2000-0722.